NANO LETTERS

pubs.acs.org/NanoLett Letter

Simultaneous High-Strength and Deformable Nanolaminates With Thick Biphase Interfaces

Justin Y. Cheng, Shuozhi Xu, Youxing Chen, Zezhou Li, Jon K. Baldwin, Irene J. Beyerlein, and Nathan A. Mara*

Cite This: *Nano Lett.* 2022, 22, 1897−1904 Read Online

ACCESS | Metrics & More | Article Recommendations | Supporting Information

ABSTRACT: Two-phase nanolaminates are known for their high strength, yet they suffer from loss of ductility. Here, we show that broadening heterophase interfaces into "3D interfaces" as thick as the individual layers breaks this strength-ductility trade-off. In this work, we use micropillar compression and transmission electron microscopy to examine the processes underlying this breakthrough mechanical performance. The analysis shows that the 3D interfaces stifle flow instability via shear band formation through their interaction with dislocation pileups. To explain this observation, we use phase field dislocation dynamics (PFDD) simulations to study the interaction between a pileup and a 3D interface. Results show that when dislocation pileups fall below a characteristic size relative to the 3D interface thickness, transmission across interfaces becomes significantly frustrated. Our work demonstrates that 3D interfaces attenuate pileup-induced stress concentrations, preventing shear localization and offering an alternative way to enhanced mechanical performance.

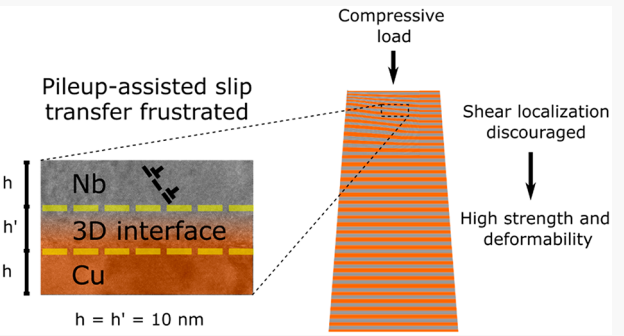

KEYWORDS: *nanomaterials, strength, dislocations, toughness, interfaces, composite*

Metallic nanostructured composites draw considerable interest due to exceptionally high strength and hardness; however, they tend to also suffer from limited deformability, giving rise to the "strength-ductility trade-off".[1] This trade-off is rooted in defect-interface interactions, where microstructural features, such as grain boundaries, limit plastic deformation before onset of shear localization or fracture.[1−4] Many approaches attempt to circumvent this limitation, such as introducing gradient nanostructures[5] or encouraging phase transformation-induced plasticity.[6] The current work overcomes this trade-off by introducing three-dimensional (3D) interfaces into a two-phase nanocomposite. Unlike conventional two-dimensional (2D) interfaces, 3D interfaces extend into the dimension normal to the interface plane and are chemically and crystallographically divergent from the two phases they join. Although this approach has been explored before in some sense using homogeneous amorphous interfacial regions,[7,8] here we exert control over interfacial heterogeneities on the length scale of a few nanometers in all spatial dimensions to yield improved mechanical properties. Using Cu/Nb nanolaminates as a model system, we probe the mechanical behavior arising from 3D interfaces with thickness comparable to that of the pure Cu and Nb layers. At this relative length scale, 3D interfaces confer both strength and deformability by discouraging plasticity-limiting shear localization. Deformability is defined here as strain prior to the onset of a strain-softening shear localization. We present an interface-dislocation pileup mediated deformation mechanism in which the relative scale between pure metal layer and interface thicknesses plays a crucial role in suppressing shear localization. We simulate the collective movement of pileup dislocations across a 3D interface under quasistatic loading and with atomically informed phase field dislocation dynamics (PFDD). PFDD is uniquely able to simulate the minimum energy pathway taken by arrays of dislocations across 3D interfaces. This work uncovers a key microstructural metric for controlling 3D interface structure in nanocomposites to achieve record combinations of strength and plasticity by encouraging delocalized deformation.

Previous studies on nanolaminates established that at layer thicknesses below ∼100 nm, strength rises to near-theoretical levels.[9−16] In this regime, interface content is high and so material response is dominated by the structure of heterophase interfaces.[17] Because our thin film synthesis method provides a narrow and controllable distribution of interface structures, it

Received: October 26, 2021
Revised: February 14, 2022
Published: February 21, 2022

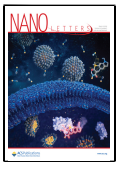

https://doi.org/10.1021/acs.nanolett.1c04144
Nano Lett. 2022, 22, 1897−1904

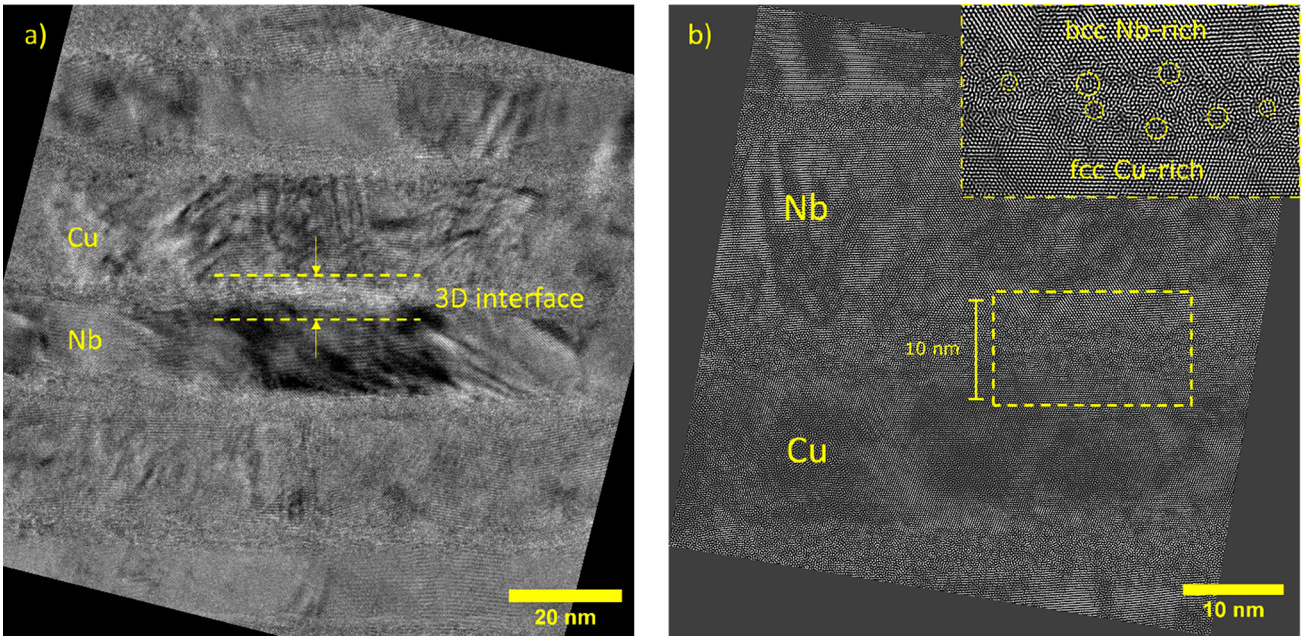

Figure 1. Bright-field cross-sectional TEM micrographs of 10-10 Cu/Nb. (a) Difference in diffraction contrast caused by crystallographic heterogeneities in the 3D interfaces between Cu and Nb. Regions that are crystallographically distinct from pure material appear thinner than 10 nm. This is because alloyed material that is deposited in a composition close to pure material tends to adopt the crystal structure of that material due to epitaxy. (b) Fourier-filtered high-resolution micrograph highlighting crystallographic heterogeneities on the length scale of a few unit cells. The inset is a magnified region in the micrograph; local regions containing many such heterogeneities are outlined by yellow circles.

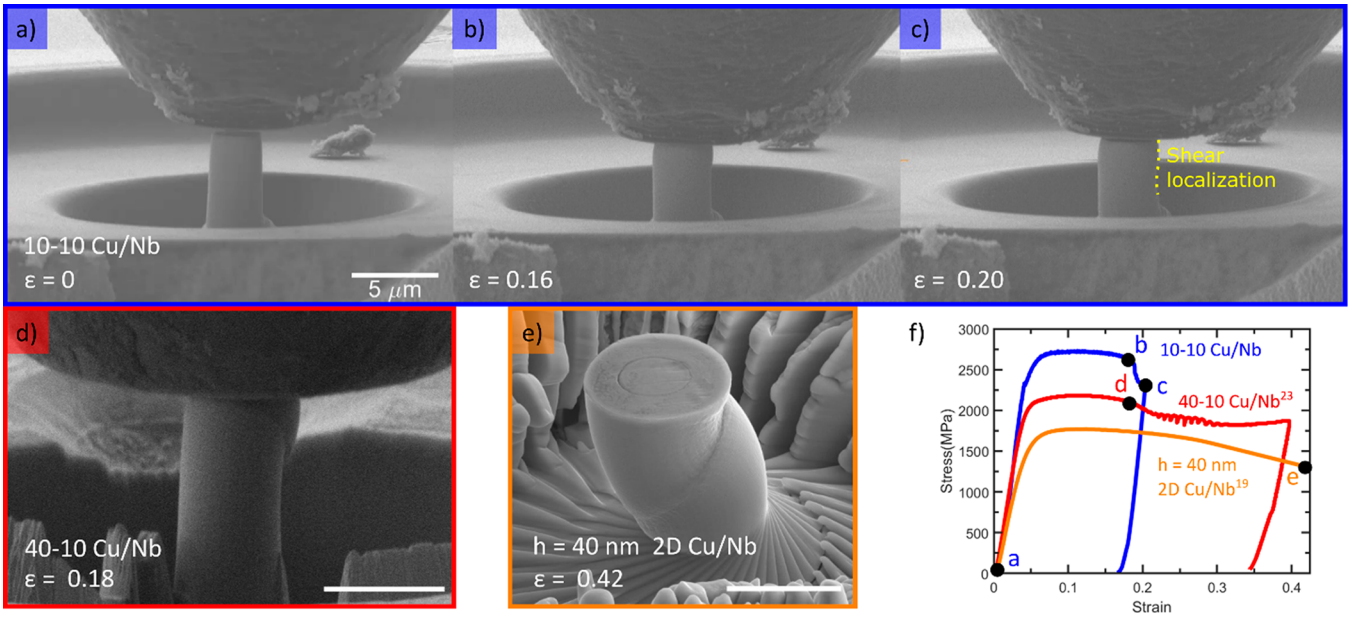

Figure 2. Snapshots of the compressed 10-10 Cu/Nb micropillar: (a) before compression, (b) during homogeneous deformation, and (c) after shear localization. For comparison, we have included a snapshot of 40-10 Cu/Nb at a comparable strain to (b) in (d), as well as a micrograph of h = 40 nm 2D Cu/Nb in (e) after *ex situ* compression. It can be seen in (d) and (f) that 40-10 Cu/Nb shear localizes prior to the strains indicated in (b) and (d), and it does so very severely. Stresses are corrected for taper in the cases of 10-10 Cu/Nb and h = 40 nm 2D Cu/Nb (see Supporting Information for further details), while they are simply engineering for 40-10 Cu/Nb. Strains presented are engineering. All scale bars represent equal lengths. Panel e reprinted from ref 19 with permission. Copyright 2010 AIP Publishing.

offers a unique opportunity to systematically investigate the influence of interface structure on mechanical behavior. Cu/Nb nanolaminates (hereafter Cu/Nb) have evolved as a model system for studying the influence of processing-dependent interface structure on dislocation motion and the resulting impact on mechanical properties.[11,18−21] The positive mixing enthalpy of Cu and Nb lead these interfaces to be atomically sharp. Depending on processing method, Cu/Nb nanolaminates may possess a particular interface structure that prevails throughout the material. Abrupt Cu/Nb interfaces promote mechanisms leading to an early onset of flow instability.[22] Here, we show that super thick 3D interfaces whose thickness equals the pure layer thickness discourage

https://doi.org/10.1021/acs.nanolett.1c04144
Nano Lett. 2022, 22, 1897−1904

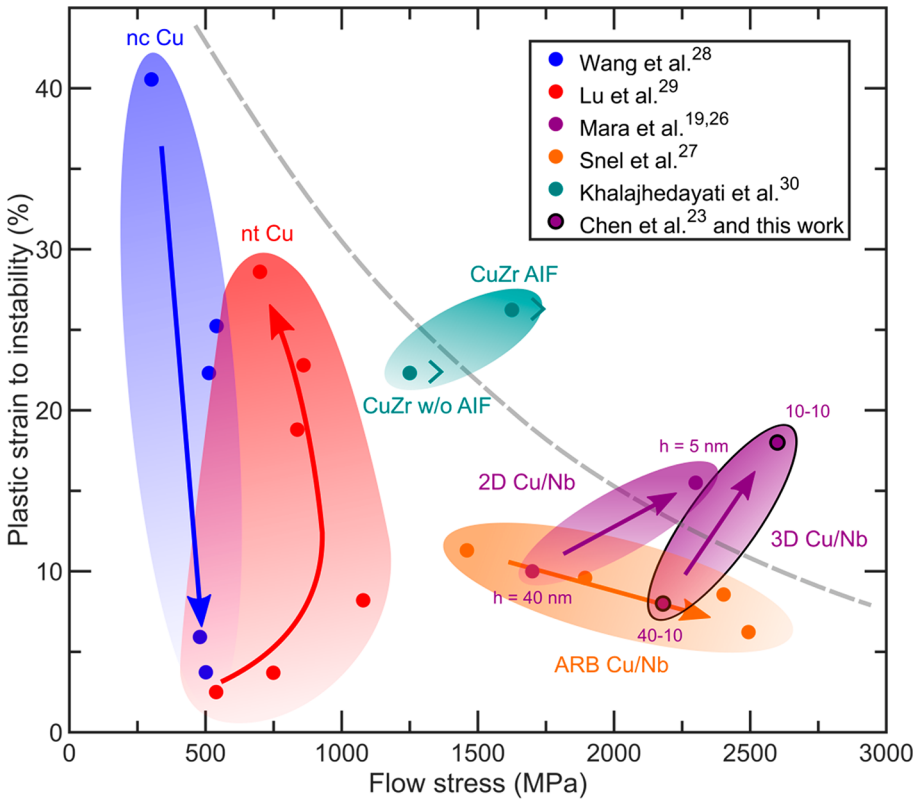

Figure 3. Plastic strain at onset of plastic instability plotted against flow stress for nanocrystalline (nc) and nanotwinned (nt) Cu, PVD and ARB 2D Cu/Nb, CuZr alloy, and 3D Cu/Nb. Arrows indicate decreasing dislocation obstacle spacing (other dislocations, grain boundaries, twin boundaries, or heterophase interfaces). There is no arrow for CuZr, since properties are solely enhanced by introduction of AIFs (not by a change in obstacle spacing). Chevrons are also included for CuZr alloys to denote that deformability may be higher than indicated; *in situ* footage was not available or tests were terminated prior to shear localization. Note that in both PVD 2D and 3D Cu/Nb, strength and plasticity do not exhibit a trade-off as layer thickness decreases. Below the dashed line, materials undergo the strength-ductility trade-off. These data comprise a mix of tensile and compressive tests and all stress and strain values are true (converted from engineering where necessary).

plastic instability without sacrificing strength, thereby breaking the strength-ductility trade-off.

We introduce substantially thick 3D interfaces between Cu and Nb layers to create "3D Cu/Nb" using DC magnetron sputtering physical vapor deposition (PVD). We modulate Cu and Nb sputter rates smoothly between deposition of pure layers. This process results in chemically and crystallographically heterogeneous, few nanometers-wide regions in the 3D interface (Figure 1 and Figure S1). This process has been used before to create 3D Cu/Nb with pure-metal layer thickness, h, of 40 nm and 3D interface thickness, h', of 10 nm (40-10 Cu/Nb).[23] To test the extreme in interface thickness, we create a Cu/Nb nanolaminate with h = 10 nm and h' = 10 nm (10-10 Cu/Nb). Three-dimensional interface structures differ from the one-to-few atoms thick, "2D interfaces", found in Cu/Nb nanolaminates described extensively in the literature.[20]

In situ SEM micropillar compression normal to the interfaces was conducted on FIB-machined pillars. Here we use compressive strain to plastic instability as an indicator of ability to homogeneously deform before shear softening and rupturing. In the context of the strength-ductility trade-off, this is a measure of ductility in the absence of stress concentrators such as the neck that commonly forms during tensile testing. Figure 2 shows movie snapshots of a micropillar before and during deformation, along with a representative stress−strain curve. Details on stress calculation and experimental considerations for FIB fabricated pillars are found in the Supporting Information,[24,25] while videos of compression tests conducted on 10-10 and 40-10 Cu/Nb are included as Supporting Information Videos 1 and 2, respectively. To ensure repeatability, we conduct three compression tests for each condition for 10-10 Cu/Nb. Yield stress for these pillars is 2100 ± 100 MPa via deviation from linearity and the ultimate compressive stress is 2500 ± 70 MPa. Engineering plastic strain to failure is 16 ± 2%, where failure is defined as a gross shape change in the pillar corresponding to a significant stress drop. This criterion is chosen because if more stress were to be applied to the material, it would deform until rupture. Remarkably, 10-10 Cu/Nb work hardens enough to resist plastic instability until 16% strain, suggesting that it resists the formation of strain-softening shear localizations that otherwise readily form in 2D interface Cu/Nb (hereafter 2D Cu/Nb).[19] Also of note is the high yield stress compared to that of 2D Cu/Nb (~2000 MPa) despite a lower h of 5 nm.[26]

We observe that 10-10 Cu/Nb is stronger and more deformable than 40-10 Cu/Nb[23] but with the added benefit that 10-10 Cu/Nb can be homogeneously strained to a higher extent. Yield is defined as the stress and strain at which a line fit to the linear portion of the stress strain curve deviates from the curve by 5% in stress. From Figure 2 and *in situ* footage, the yield stress is lower for a higher h in 40-10 (1900 MPa) than for 10-10 Cu/Nb. The *in situ* footage of pillar compression of the 10-10 and 40-10 3D Cu/Nb nanolaminates

https://doi.org/10.1021/acs.nanolett.1c04144
Nano Lett. 2022, 22, 1897−1904

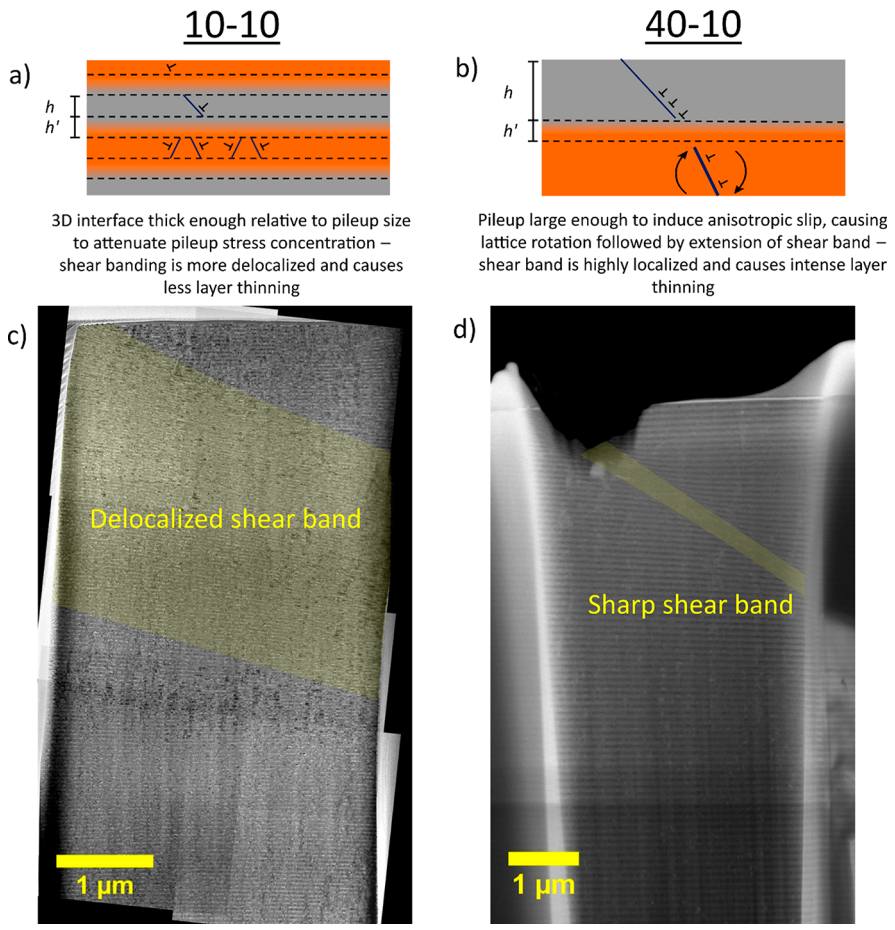

Figure 4. Diagrams depicting hypothesized dislocation pileup-interface interactions in (a) 10-10 and (b) 40-10 Cu/Nb. (a) Effect of limited pileup size relative to 3D interface thickness—slip transfer is stifled enough to inhibit formation of a highly localized shear band. (b) Pileup sizes are large enough to encourage slip transfer along common slip systems across pure metal layers, facilitating formation of a sharp shear band. The proposed pileup-interface interactions are borne out by the nature of deformation observed in TEM micrographs of highly deformed pillars in (c) 10-10 and (d) 40-10 Cu/Nb.

reveals that uniform deformation ends with the formation of a shear band. Shear localization initiates earlier in the 40-10 (~10%) sample than in the 10-10 (12%) one (Figure S3). Additionally, the shear band formed in the 10-10 is less abrupt than that found in 40-10 (Figure 2d). Comparison between these two 3D Cu/Nb nanocomposites demonstrates that increasing h' relative to h further improves mechanical performance.

Increasing deformability with finer nanoscale layer thickness is counterintuitive since most nanolayered materials become more prone to strain localization as layer thickness reduces and strength increases. Here, the flow stress at onset of shear localization and the extent of homogeneous plastic strain are plotted in Figure 3 for 3D Cu/Nb and a variety of related materials, including 2D Cu/Nb made via PVD[19,26] and ARB,[27] nanocrystalline (nc)[28] and nanotwinned (nt) Cu,[29] and CuZr nanostructured alloys.[30] For Cu/Nb, onset of shear localization is defined by an abrupt change in pillar shape concurrent with a significant drop in flow stress. In nanostructured materials that do not display such instability, such as nc or nt Cu, the onset of shear localization is taken as the strain at which ultimate tensile/compressive stress occurs. In most nanocrystalline metals like nc Cu and nt Cu, flow stress is enhanced at the expense of plasticity by decreasing the mean distance between dislocation obstacles. This distance is dictated by grain size (nc Cu), twin boundary spacing (nt Cu), or layer thickness (ARB Cu/Nb). In the other nanostructured materials with controlled interfaces mentioned, there is no such trade-off between flow stress and strain to shear instability. 3D Cu/Nb falls in the latter category, constituting an optimal combination of microstructural length scales to achieve strength and deformability. A lesser drop in layer thickness in 3D Cu/Nb is required to achieve comparable improvements in strength and deformability as compared to 2D Cu/Nb. This remarkable behavior demands an investigation into the physics underlying the deformation mechanisms observed during and after *in situ* micropillar compression.

As shear banding limits deformability in both 3D and 2D Cu/Nb nanocomposites, discussion of its progression in 2D Cu/Nb illuminates why shear banding is postponed and less severe in 3D Cu/Nb. 2D Cu/Nb showed that shear band formation in Cu/Nb requires shear transmission across multiple layers along a common plane (Figure 2e).[19] Dislocation-mediated shear transmission across Cu−Nb interfaces is not energetically favorable at the onset of plastic deformation.[31] Thus, shear transmission must be preceded by other modes of deformation, such as slip-induced lattice rotation in Cu and Nb grains toward geometrically favored, well-aligned slip planes.[19,23] Once lattice rotation proceeds to a sufficient extent, mechanisms such as interfacial sliding or

https://doi.org/10.1021/acs.nanolett.1c04144
Nano Lett. 2022, 22, 1897−1904

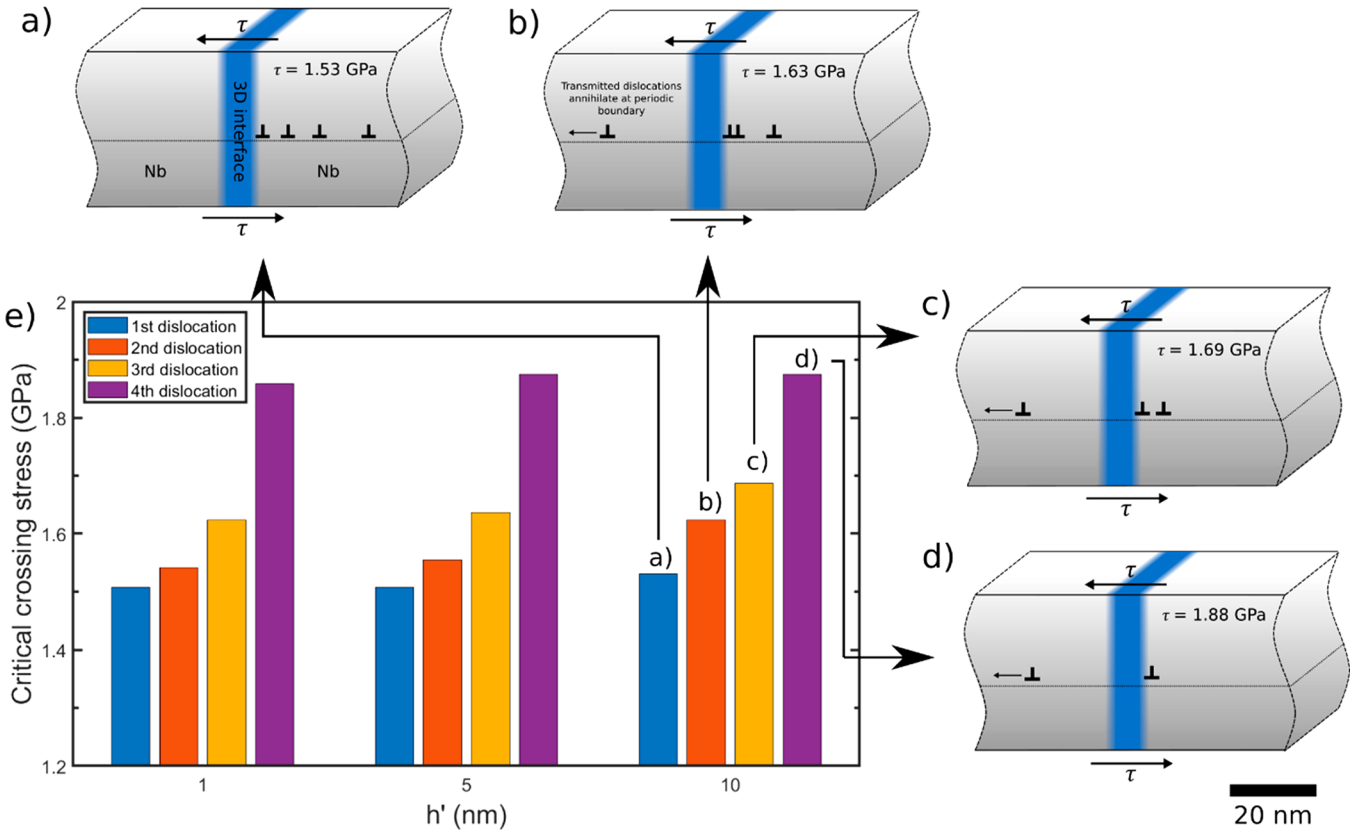

Figure 5. (a–d) A depiction of the interaction of a four dislocation-wide pileup with a 10 nm 3D interface in the PFDD model described in the text and (e) charts of stress required to transmit each dislocation in a pileup across a 3D interface, presented as a function of h' on the horizontal axis and pileup size in chart titles. The y-axis in (e) is truncated to aid in visualization of difference in dislocation transmission stresses. In (a–d), pileup dislocation positions are drawn to scale in relation to the 3D interface at the critical shear stress required to transmit the leading dislocation. The simulation box is truncated in this depiction to draw attention to details of the pileup. Dislocations are depicted under applied shear stresses of (a) 1.53, (b) 1.63, (c) 1.69, and (d) 1.88 GPa. As the stress increases, the equilibrium pileup size decreases, indicating that the stress required to induce dislocation transmission across the 3D interface is inversely proportional to the pileup size. In panel e, crossing stresses are not strongly affected by the presence of the 3D interface at diminished h' = 1 or 5 nm. However, at h' = 10 nm the mechanical advantage provided by trailing pileup dislocations is not sufficient to aid transmission of the leading pileup across the interface for the 2nd and 3rd dislocations to transmit. Crossing stresses are modestly higher for these dislocations for h' = 10 nm as compared to smaller values of h'.

concerted slip transfer across multiple layers lead to local strain softening and shear banding. The formation of plasticity-limiting shear bands can be suppressed in Cu/Nb if lattice rotation or interlayer transmission of slip are frustrated.

We hypothesize that above a critical h'/h ratio, 3D interfaces enhance mechanical properties in Cu/Nb by frustrating the ability for dislocation pileups in one pure layer to cascade dislocations across the interface to the next pure layer (Figure 4). At yield, the first dislocations activated in the Cu and Nb nanolayers pile up at the interface. In order for lattice rotation to occur in a given grain, the local stress field must be perturbed from a uniaxial stress state,[19] which occurs at sites such as pillar corners. As deformation continues, lattice rotation propagates across layers due to the influence of stress concentrations originating from dislocation pileup stress fields. Pileup stress fields in one phase directionally favor continued slip on similarly aligned slip systems in the adjoining phase. However, this interlayer lattice rotation only readily occurs if pileup stress field magnitudes are high enough for the dislocations to penetrate the 3D interface. If this is the case, then lattice rotation can propagate across multiple layers. This aligns grains across several layers favorably for slip along common slip systems, allowing the shear band to grow. The stress intensity associated with pileups is proportional to the maximum pileup size on active slip systems in Cu and Nb layers, which in turn is determined by the thickness of the layers. Thus, pileup size is substantial in layers with h = 40 nm but are limited when h = 10 nm (see Supporting Information for a supporting calculation). When the 3D interface is substantially thick in comparison to the size of pileups, slip is stymied and a shear band cannot be effectively propagated.

To understand the role that 3D interface thickness and dislocation pileup size play in deformation, we use PFDD to calculate the stress required to transmit a pile up of dislocations across the 3D interface as a function of pileup size and 3D interface thickness h'. Although only pileup size is explicitly used in the simulation, it is related to h in our experimental work, as h limits the size of pileups along Schmid-factor-favored slip planes. PFDD is a computational framework that can account for the motion of multiple dislocations in three dimensions and can be applied to morphologically and crystallographically complex structures. This particular model simultaneously incorporates elastic anisotropy, material heterogeneity, and dislocation core dissociation into the system energetics under quasistatic loading,[32] a feat that would be computationally expensive using fully atomistic methods.[33]

Our system consists of a 3D interface, idealized as BCC $Cu_{0.1}Nb_{0.9}$, sandwiched between two BCC Nb layers. Although

https://doi.org/10.1021/acs.nanolett.1c04144
Nano Lett. 2022, 22, 1897–1904

this structure is simplified compared to what is experimentally observed, it allows us to probe the related effects of pure layer thickness (proportional to dislocation pileup size) versus 3D interface thickness on the ability to attenuate slip and discourage shear banding. The boundary between Nb and the 3D interface is assumed coherent, which is reasonable considering the similar lattice parameters for Nb and the Nb-rich side of the 3D interface. The properties of the $Cu_{0.1}Nb_{0.9}$ interface required for the simulation, such as the elastic constants C_{11}, C_{12}, and C_{44}, and the generalized stacking fault energy (GSFE) curve for the {110} glide plane were calculated using molecular dynamics.[32]

Initially, stress is increased until sufficient to pile up dislocations at the 3D interface. Applying additional stress transmits the leading dislocation into the 3D interface. Once the lead dislocation is injected into the 3D interface, it glides through to the other side of the 3D interface with no additional stress increment. This represents the critical stress for dislocation transmission across the 3D interface. After the lead dislocation transmits, the pile up and associated mechanical advantage decrease, so an increased applied stress is required for the next dislocation to transmit. Figure 5a–d illustrates this phenomenon, depicting transmission of each dislocation in a four-dislocation wide pileup across a 3D interface of h' = 10 nm. As more dislocations cross the interface, the critical crossing stress increases from 1.53 to 1.88 GPa.

We conducted calculations for 3D interfaces with h' = 1, 5, and 10 nm. Although the scenario presented here is different than the experimental work presented in Figure 4, these simulations probe the same underlying concept of the role of relative length scale between the 3D interface and pileup size on transmission stress. Figure 5e shows that the critical crossing stresses for leading pileup dislocations are inversely proportional to pileup size, while they are proportional to h'. This suggests that the thicker a 3D interface is, the higher stress barrier to slip transfer it poses. The largest effect that a 3D interface has on dislocation transmission manifests for h' = 10 nm in the critical crossing stress required for transmission of the second and third pileup dislocations. From Figure 5, it can be seen that when h' = 10 nm, the crossing stress for each dislocation increases by about 100 MPa for the second and third dislocations to cross as compared to lower h'. Although it represents a small stress difference, it is enough to encourage slip activation on other slip systems with nearly the same Schmid factor. This frustrates shear band formation on slip systems shared among multiple layers, encouraging homogeneous deformation and increasing the applied stress required to plastically deform the material. Clearly, sufficiently thick 3D interfaces attenuate the stress field of piled-up dislocations, providing outsize improvements in mechanical behavior. By the time the first dislocation starts to transmit into the 3D interface, the pileup size has decreased from four to three dislocations. At h' = 10 nm, the 3D interface is thick enough compared to the pileup size to substantially reduce the mechanical advantage toward dislocation transmission. A similar sequence of events follows when the second dislocation begins to transmit. These results support our hypothesis that in 10-10 Cu/Nb, restricted pileup size relative to h' necessitates large stresses for dislocations to cross 3D interfaces, stopping slip localizations from traversing several layers. In contrast, in the 40-10 Cu/Nb nanolaminate, substantial pileups form, causing multilayer slip transfer and shear band propagation at lower stress and strain. In short, our experimental and simulation results show that 3D interface-pileup dislocations hinge on the same metric. The relative scale between maximum pileup size allowed by h and 3D interface thickness h' determines whether interlayer slip is frustrated. Thus, h'/h ratio is the underpinning microstructural metric that determines mechanical behavior in 3D interface materials.

In summary, we show in this work that appropriately dimensioned 3D interfacial regions between crystalline regions in laminated Cu/Nb nanocomposites simultaneously increase strength and deformability while decreasing the tendency for shear localization. Combining experiments and simulations, we show that this unusual behavior arises from a special interaction of pileups with 3D interfaces and depends on the interface thickness-to-pileup size ratio, which when sufficiently high attenuates the mechanical advantage that pileups provide to dislocation transmission across the interface. Substantially thick 3D interfaces drive up yield stress of the composite which in turn activates slip on nongeometrically favored planes. This dispersion of slip can result in homogeneous deformation, increasing overall deformability and work hardenability. This work uncovers a key microstructural metric that determines how much 3D interfaces enhance strength and deformability in nanocrystalline alloys, paving the way for ultrastrong yet deformable materials.

MATERIALS AND METHODS

3D Cu/Nb metallic multilayers were synthesized using DC magnetron sputtering onto a rotating (100) Si substrate with native oxide at room temperature under 3 mTorr Ar. Pure metal layers were deposited with 150 W Cu and 400 W Nb target power to achieve a deposition rate of 3 Å/s. 3D interfaces were synthesized by linearly ramping Cu and Nb targets in opposing directions from full power to no power. Micropillars and TEM-transparent lamella were fabricated in an FEI Helios NanoLab G4 FIB/SEM. Compression of pillars was conducted using a Bruker Hysitron PI 88 *in situ* picoindenter in the aforementioned FIB/SEM. These tests were carried out in displacement control at an initial engineering strain rate of 10^{-4}/s. Conventional TEM, STEM, and HRTEM were conducted in a FEI Titan and a Thermo Fisher Talos FX200. The PFDD model used is described in the Supporting Information and the work of Xu et al.[32]

ASSOCIATED CONTENT

Supporting Information

The Supporting Information is available free of charge at https://pubs.acs.org/doi/10.1021/acs.nanolett.1c04144.

Contains in-detail discussion of experimental methods and theoretical computations used in the main text (PDF)

In situ micropillar compression footage of 10-10 Cu/Nb (MP4)

In situ micropillar compression footage of 40-10 Cu/Nb (MP4)

AUTHOR INFORMATION

Corresponding Author

Nathan A. Mara − *Department of Chemical Engineering and Materials Science, University of Minnesota Twin Cities, Minneapolis, Minnesota 55455, United States*;
Email: mara@umn.edu

https://doi.org/10.1021/acs.nanolett.1c04144
Nano Lett. 2022, 22, 1897−1904

Authors

Justin Y. Cheng − *Department of Chemical Engineering and Materials Science, University of Minnesota Twin Cities, Minneapolis, Minnesota 55455, United States;* orcid.org/0000-0002-2339-1142

Shuozhi Xu − *Department of Mechanical Engineering, University of California, Santa Barbara, California 93106-5070, United States*

Youxing Chen − *Mechanical Engineering and Engineering Science, University of North Carolina, Charlotte, North Carolina 28223-0001, United States*

Zezhou Li − *Department of Chemical Engineering and Materials Science, University of Minnesota Twin Cities, Minneapolis, Minnesota 55455, United States*

Jon K. Baldwin − *Center for Integrated Nanotechnologies, Los Alamos National Laboratory, Los Alamos, New Mexico 87545, United States*

Irene J. Beyerlein − *Department of Mechanical Engineering, University of California, Santa Barbara, California 93106-5070, United States; Materials Department, University of California, Santa Barbara, California 93106-5050, United States*

Complete contact information is available at: https://pubs.acs.org/10.1021/acs.nanolett.1c04144

Notes

The authors declare no competing financial interest.

■ ACKNOWLEDGMENTS

This work is supported by DOE BES DE-SC0020133 Office of Science, Basic Energy Sciences. J.Y.C. is supported in part by DOE NNSA SSGF under cooperative agreement number DE-NA0003960. Parts of this work were carried out in the Characterization Facility, University of Minnesota, which receives partial support from NSF through the MRSEC program. The authors acknowledge the Minnesota Supercomputing Institute (MSI) at the University of Minnesota for providing resources that contributed to the research results reported within this paper. Use was made of computational facilities purchased with funds from the National Science Foundation (CNS-1725797) and administered by the Center for Scientific Computing (CSC). The CSC is supported by the California NanoSystems Institute and the Materials Research Science and Engineering Center (MRSEC; NSF DMR 1720256) at UC Santa Barbara. This work was performed, in part, at the Center for Integrated Nanotechnologies, an Office of Science User Facility operated for the U.S. Department of Energy (DOE) Office of Science by Los Alamos National Laboratory (Contract 89233218CNA000001) and Sandia National Laboratories (Contract DE-NA-0003525). Special thanks to Nan Li for providing 40-10 Cu/Nb data.

■ REFERENCES

(1) Koch, C. C.; Morris, D. G.; Lu, K.; Inoue, A. Ductility of nanostructured materials. *MRS Bull.* **1999**, *24*, 54−58.

(2) Ma, E.; Zhu, T. Towards strength−ductility synergy through the design of heterogeneous nanostructures in metals. *Mater. Today* **2017**, *20*, 323−331.

(3) Li, Z.; et al. Regain Strain-Hardening in High-Strength Metals by Nanofiller Incorporation at Grain Boundaries. *Nano Lett.* **2018**, *18*, 6255−6264.

(4) Narayanan, S.; Cheng, G.; Zeng, Z.; Zhu, Y.; Zhu, T. Strain Hardening and Size Effect in Five-fold Twinned Ag Nanowires. *Nano Lett.* **2015**, *15*, 4037−4044.

(5) Cao, P. The Strongest Size in Gradient Nanograined Metals. *Nano Lett.* **2020**, *20*, 1440−1446.

(6) Ma, E. Eight routes to improve the tensile ductility of bulk nanostructured metals and alloys. *JOM* **2006**, *58*, 49−53.

(7) Vo, N. Q.; Averback, R. S.; Ashkenazy, Y.; Bellon, P.; Wang, J. Forced chemical mixing at Cu-Nb interfaces under severe plastic deformation. *J. Mater. Res.* **2012**, *27*, 1621−1630.

(8) Fan, Z.; et al. Unusual size dependent strengthening mechanisms of Cu/amorphous CuNb multilayers. *Acta Mater.* **2016**, *120*, 327−336.

(9) Misra, A.; et al. Structure and mechanical properties of Cu-X (X = Nb,Cr,Ni) nanolayered composites. *Scr. Mater.* **1998**, *39*, 555−560.

(10) Misra, A.; Kungg, H. Deformation Behavior of Nanostructured Metallic Multilayers. *Adv. Eng. Mater.* **2001**, *3*, 217−222.

(11) Misra, A.; Hirth, J. P.; Hoagland, R. G. Length-scale-dependent deformation mechanisms in incoherent metallic multilayered composites. *Acta Mater.* **2005**, *53*, 4817−4824.

(12) Mara, N. A.; Beyerlein, I. J. Review: Effect of bimetal interface structure on the mechanical behavior of Cu-Nb fcc-bcc nanolayered composites. *J. Mater. Sci.* **2014**, *49*, 6497−6516.

(13) Demkowicz, M. J.; Thilly, L. Structure, shear resistance and interaction with point defects of interfaces in Cu-Nb nanocomposites synthesized by severe plastic deformation. *Acta Mater.* **2011**, *59*, 7744−7756.

(14) Beyerlein, I. J.; Demkowicz, M. J.; Misra, A.; Uberuaga, B. P. Defect-interface interactions. *Prog. Mater. Sci.* **2015**, *74*, 125−210.

(15) Wang, J.; Hoagland, R. G.; Hirth, J. P.; Misra, A. Atomistic modeling of the interaction of glide dislocations with 'weak' interfaces. *Acta Mater.* **2008**, *56*, 5685−5693.

(16) Misra, A.; Hirth, J. P.; Hoagland, R. G.; Embury, J. D.; Kung, H. Dislocation mechanisms and symmetric slip in rolled nano-scale metallic multilayers. *Acta Mater.* **2004**, *52*, 2387−2394.

(17) Anderson, P. M.; Foecke, T.; Hazzledine, P. M. Dislocation-based deformation mechanisms in metallic nanolaminates. *MRS Bull.* **1999**, *24*, 27−33.

(18) Yu-Zhang, K.; Embury, J. D.; Han, K.; Misra, A. Transmission electron microscopy investigation of the atomic structure of interfaces in nanoscale Cu-Nb multilayers. *Philos. Mag.* **2008**, *88*, 2559−2567.

(19) Mara, N. A.; Bhattacharyya, D.; Hirth, J. P.; Dickerson, P.; Misra, A. Mechanism for shear banding in nanolayered composites. *Appl. Phys. Lett.* **2010**, *97*, No. 021909.

(20) Beyerlein, I. J.; et al. Structure−Property−Functionality of Bimetal Interfaces. *JOM* **2012**, *64*, 1192−1207.

(21) Beyerlein, I. J.; et al. Interface-driven microstructure development and ultra high strength of bulk nanostructured Cu-Nb multilayers fabricated by severe plastic deformation. *J. Mater. Res.* **2013**, *28*, 1799−1812.

(22) Zheng, S. J. J.; et al. Plastic instability mechanisms in bimetallic nanolayered composites. *Acta Mater.* **2014**, *79*, 282−291.

(23) Chen, Y.; et al. Effects of three-dimensional Cu/Nb interfaces on strengthening and shear banding in nanoscale metallic multilayers. *Acta Mater.* **2020**, *199*, 593−601.

(24) Hütsch, J.; Lilleodden, E. T. The influence of focused-ion beam preparation technique on microcompression investigations: Lathe vs. annular milling. *Scr. Mater.* **2014**, *77*, 49−51.

(25) Nix, W. D.; Greer, J. R.; Feng, G.; Lilleodden, E. T. Deformation at the nanometer and micrometer length scales: Effects of strain gradients and dislocation starvation. *Thin Solid Films* **2007**, *515*, 3152−3157.

(26) Mara, N. A.; Bhattacharyya, D.; Dickerson, P.; Hoagland, R. G.; Misra, A. Deformability of ultrahigh strength 5nm Cu/Nb nanolayered composites. *Appl. Phys. Lett.* **2008**, *92*, 231901.

(27) Snel, J.; et al. Deformation Mechanism Map of Cu/Nb Nanoscale Metallic Multilayers as a Function of Temperature and Layer Thickness. *JOM* **2017**, *69*, 2214−2226.

(28) Wang, Y.; Chen, M.; Zhou, F.; Ma, E. High tensile ductility in a nanostructured metal. *Nature* **2002**, *419*, 912−915.
(29) Lu, K.; Lu, L.; Suresh, S. Strengthening Materials by Engineering Coherent Internal Boundaries at the Nanoscale. *Science* **2009**, *324*, 349−352.
(30) Khalajhedayati, A.; Pan, Z.; Rupert, T. J. Manipulating the interfacial structure of nanomaterials to achieve a unique combination of strength and ductility. *Nat. Commun.* **2016**, *7*, 10802.
(31) Wang, J.; Hoagland, R. G.; Hirth, J. P.; Misra, A. Atomistic simulations of the shear strength and sliding mechanisms of copper-niobium interfaces. *Acta Mater.* **2008**, *56*, 3109−3119.
(32) Xu, S.; Cheng, J. Y.; Li, Z.; Beyerlein, I. J.; Mara, N. A. Phase-field modeling of the interactions between an edge dislocation and an array of obstacles. *Comput. Methods Appl. Mech. Eng.* **2022**, *389*, 114426.
(33) Beyerlein, I. J.; Hunter, A. Understanding dislocation mechanics at the mesoscale using phase field dislocation dynamics. *Philos. Trans. R. Soc. A Math. Phys. Eng. Sci.* **2016**, *374*, 20150166.

https://doi.org/10.1021/acs.nanolett.1c04144
Nano Lett. 2022, 22, 1897−1904